

Research on measurement method of grinding wheel profile based on image mosaic

Tianyi Li[✉], Zhongjun Qiu¹ and Junjie Tang

State Key Laboratory of Precision Measuring Technology and Instruments, Tianjin University, Tianjin 300072, People's Republic of China

E-mail: qiuzhongjun@tju.edu.cn

Received 26 September 2019, revised 14 November 2019

Accepted for publication 19 November 2019

Published 31 December 2019



Abstract

Grinding is one of the most effective processing methods of hard and brittle materials. In the grinding process, measurement of the grinding wheel profile is of great significance for evaluating the grinding wheel processing accuracy, detecting wear and compensating machining errors. In this paper, a novel grinding wheel profile measurement method based on an image mosaic is proposed to realize fast non-contact profile measurement. A profile template matching approach based on the profile search algorithm is constructed according to the characteristics of the wheel profile, and the complete grinding wheel profile is obtained and measured by a fast and accurate mosaic of profile images. The experimental results show that the proposed algorithm is more efficient and accurate compared with the traditional image mosaic algorithm. On the basis of this method, a measurement system for the grinding wheel profile is established and cylindrical and hemispherical grinding wheels are measured. The high-resolution complete cross-sectional profiles are obtained and the results are compared with a 2D laser profiler. The root mean squared error of the cylindrical grinding wheel is 0.08%–0.1% of the nominal radius. The center position deviation of the hemispherical grinding wheel is between $\pm 3 \mu\text{m}$ and the radius deviation is below 0.08% of the nominal radius. The measurement results indicate the feasibility and precision of this method, which can realize non-contact rapid measurement of the grinding wheel profile.

Keywords: grinding, grinding wheel, profile measurement, image mosaic

(Some figures may appear in colour only in the online journal)

1. Introduction

Grinding is one of the most effective processing methods of hard and brittle materials [1]. In the grinding process, the profile parameters of the grinding wheel directly affect the shape accuracy of workpiece [2–4]. Particularly in the grinding process of complex surfaces, such as off-axis aspherical surfaces and free-form surfaces, diamond grinding wheels not only rotate about the rotating axis at high speed, but also need to swing around their own swing center [5]. However, current grinding wheel profile measurement and evaluation

often neglects the swing process and focuses on the grinding wheel profile rotating about the central axis, which leads to an incomplete evaluation of the profile. There are still currently some limitations and shortcomings in the methods and instruments available for grinding wheel profile measurement. Therefore, it is urgent to develop a method to obtain complete profiles of the working parts of grinding wheels with different shapes to evaluate their processing accuracy, detecting wear [6] and compensating machining errors [2] in the actual grinding process.

At present, research on grinding wheel measurement mostly focuses on the measurement and characterization of the surface topography [7–9]. In particular, Brown *et al* [10]

¹ Author to whom any correspondence should be addressed.

studied multiscale analyses and characterizations of surface topographies, and synthesized a system for the organization and designation of multiscale analyses, which provides great value for evaluating the surface topography of a grinding wheel. However, there is relatively less research on the measurement of the grinding wheel profile, which is more macroscopic than the surface topography. The measurement of grinding wheel profiles mainly includes indirect measurement, contact measurement and non-contact measurement. Some studies have looked at the acquiring approach of the grinding wheel profile information by scholars.

Huang *et al* [2] employed a profilometer to measure the profile of a graphite disc ground by a grinding wheel and indirectly obtained the grinding wheel profile error, which was compensated for in the following processing. Su *et al* [11] and Chen *et al* [12] duplicated the profile of a saucer grinding wheel on a sample workpiece and a thin plate specimen respectively, and both studies used machine vision to measure the 2D profile of the specimen. The profile information of the saucer grinding wheel arc edge was indirectly acquired.

The indirect measuring method, by duplicating the profile of the grinding wheel on the specimen, is mainly used to detect wear and acquire 2D information of the saucer wheel arc edge. However, this method can only measure the cutting edge of a particular grinding wheel, and only obtain the most protruding profile of the grinding wheel, which fails to evaluate the profile at different cross-sections completely and precisely. Therefore, some direct measurement methods for the profile have also been proposed by researchers, which mainly include contact and non-contact measurement.

Magdziak *et al* [13] employed a coordinate measuring machine to measure the profile of a grinding wheel and concluded that the contact method presented a lack of repeatability, which is associated with the different measurement parameters applied during coordinate measurements.

Contact measurement acquires profile information by point contact through probe or stylus and the measuring efficiency is greatly reduced. In addition, due to the size effect and shape effect of the probe and the complex topography formed by abrasive grains, pores, and bonds, the feature points which characterize the variation of grinding wheel profile may be lost [14]. Meanwhile, the high hardness abrasive grains will inevitably cause probe or stylus wear, which will also increase the costs and affect the measurement accuracy.

With the rapid development of optical measuring and machine vision technology, non-contact measurement has been applied to the measurement of the grinding wheel profile. Valio *et al* [15] employed a 2D laser micrometer to perform on-machine macro-geometric measurement and analysis of cylindrical grinding wheel. Young *et al* [16] designed an online grinding wheel dressing system and measured the arc edge geometric dimensions of a saucer grinding wheel using autofocus and image processing technology. Xu *et al* [17] proposed a method for immediate detection of wheel wear based on image processing and extract the actual and theoretical positions of the grinding point. On this basis, the arc edge contour error of a double-bevel wheel is calculated and the wear of the corresponding grinding point can be detected online.

Non-contact measurement has many advantages; it can quickly acquire a great deal of grinding wheel profile information and avoid wear of the grinding wheel and measuring tool. However, at present, the type of grinding wheel measured by non-contact profile detection method is usually specific, such as a saucer grinding wheel or cylindrical wheel, and merely focuses on the 2D profile which rotates about the axis. Furthermore, the measuring information can be limited by camera field of view (FOV) and instrument measuring range when the measurement resolution is required to be high. The whole profile information of the grinding wheel may therefore not be acquired completely, such as in the case of a larger cylindrical grinding wheel or spherical grinding wheel, which causes incomplete evaluation of the profile.

As described above, the existing measurement methods for a grinding wheel profile all have limitations to a certain extent. At present, a direct, efficient, non-contact and more general profile measurement method for grinding wheels of different shapes and sizes is desperately needed, and then the complete profile parameters can be evaluated. In this paper, a method based on machine vision to extract point clouds of profiles of grinding wheels is proposed and used to realize the measurement and evaluation of various profiles. Combined with autofocus [18] and image processing, the complete profile is obtained by accurately mosaicing the profile images with the overlapping areas. The point cloud of the grinding wheel profile can be obtained and the profile parameters can be evaluated. This method solves the problem of indirect measurement being unable to truly reflect the grinding wheel profile; it has higher efficiency and causes no damage unlike contact measurement; it also overcomes the limitation of fixed FOV as well as the size and shape of the measured grinding wheel, which other measurement methods based on machine vision have.

2. Methodology

2.1. Measuring process

The measurement object in this paper is the profile of the grinding wheel. The combination of telecentric back light illumination and a telecentric lens is frequently used in profile measurement. Grinding wheels are opaque objects with large depths, and this type of illumination produces very sharp edges on the silhouette without refraction or reflection of abrasive grains. Furthermore, because the telecentric lens is used, there are no perspective distortions in the images. Therefore, in this study, the profile images are acquired by a background telecentric illuminator and a CCD camera from the cross-sectional direction, and these images are mosaiced to obtain the complete profile. As shown in figure 1, the whole measurement process of the grinding wheel profile in this study can be described as follows: autofocus of the profile, acquisition of profile image, image mosaic of profile. Finally, the complete grinding wheel profile is obtained and the profile parameters are evaluated.

A schematic diagram of the actual grinding wheel profile measurement system is shown in figure 2. To extract edge profile information of the grinding wheel accurately

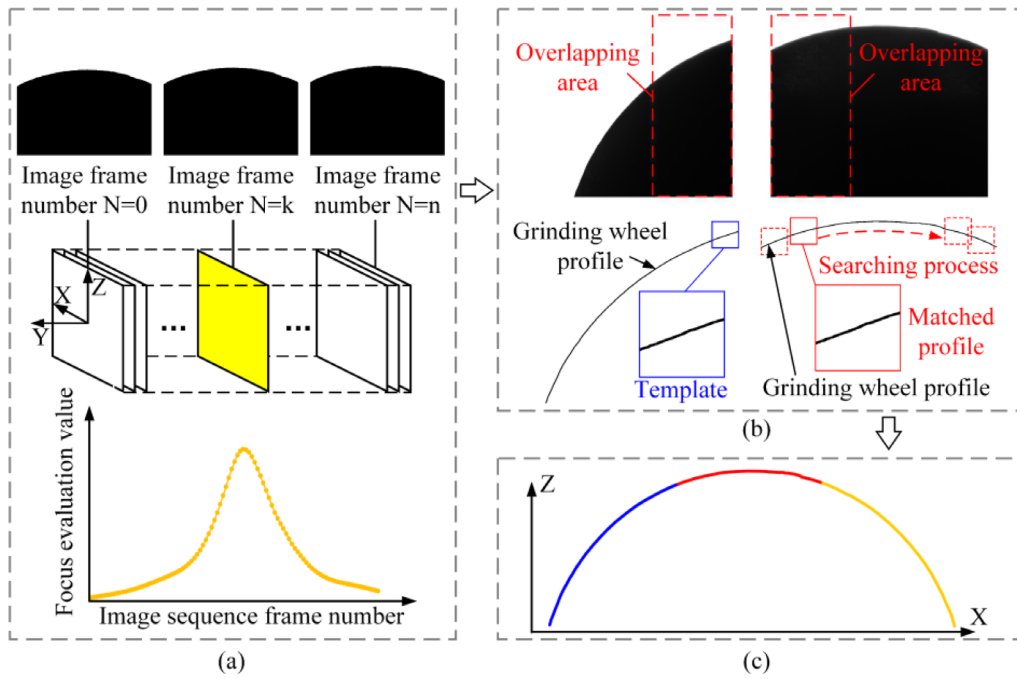


Figure 1. Grinding wheel profile measurement process: (a) autofocus process, (b) image mosaic, (c) profile measurement results.

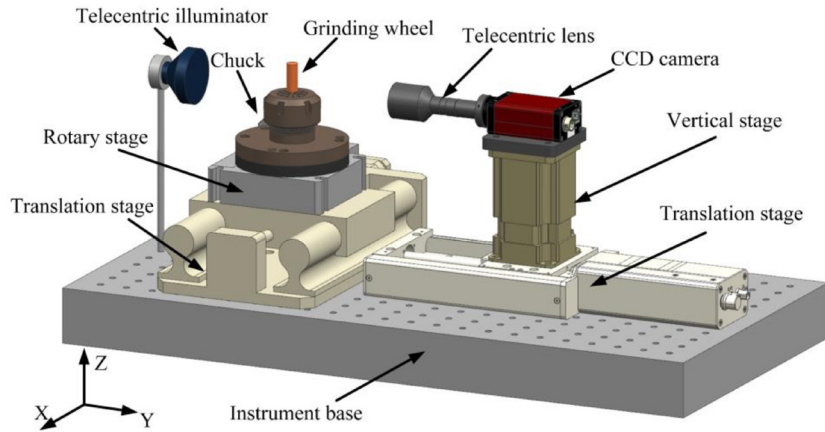


Figure 2. Schematic diagram of the actual grinding wheel profile measurement system.

from the profile images, it is necessary to focus the edge of grinding wheel through an autofocus algorithm and obtain the best-focused images. As shown in figure 2, a profile image sequence is acquired by moving the CCD camera carried by the Y-direction translation stage along the optical axis (Y axis) at equal intervals. The improved second-order difference operator is used to evaluate the sharpness of the profile image sequence, as shown in figure 1(a). By fitting the sharpness evaluation curve, the optimum focus position of the grinding wheel profile is obtained, where the best-focused profile image is captured.

A magnification telecentric lens and a high-resolution CCD camera are employed in this study to ensure the extraction accuracy of the profile point clouds. Since grinding wheels have different sizes and shapes, it is difficult to capture a complete profile in a single image. As shown in figure 1(b), when the grinding wheel profile is clearly focused, the profile

images with overlapping areas are captured in sequence by moving the X-axis translation stage and the Z-axis vertical stage, to realize relative movement perpendicular to the Y axis between the imaging system and the grinding wheel. Then the image mosaic algorithm is carried out sequentially on overlapping grinding wheel profile images for the purpose of acquiring the complete profile, which is shown in figure 1(c). In this process, a profile template matching based on the profile search algorithm is proposed, which realizes fast and accurate grinding wheel profile stitching.

By driving the rotary stage to rotate the grinding wheel, the profile images of different cross-sections are captured. Following the procedure above, profile images are mosaiced sequentially and the complete 2D grinding wheel profiles at different angles can be obtained. In the measurement process, the success of the profile image mosaic is the key to obtaining the complete profile information. In this paper, a profile

template matching based on the profile search algorithm is proposed to realize an accurate and fast mosaic of grinding wheel profile images.

2.2. Image mosaic algorithm

The image mosaic is the alignment of multiple overlapping images with a lower field of view into a larger field of view image which contains the information of all mosaic images. The image mosaic algorithm includes registration, reprojection, stitching, and blending [19, 20]. In this study, there is only a translation relationship between the grinding wheel profile images of the same cross-section and the profile is the main image information. In such conditions, finding the corresponding points between images and calculating the transformation parameters, the image mosaic can be realized through translation. Thereby, image registration becomes the key to the success of the image mosaic. This process establishes the geometric correspondence between a pair of images by finding the corresponding points in the images. With the transformation parameters, one profile image can be matched to another and stitched into a complete profile image.

The complexity of the grinding wheel surface topography results in a varied profile and each section has a unique shape. The grinding wheel profile can be extracted from a gray image and the features of one profile segment can be acquired; sequentially a profile template is established which is used to search for the same profile segment in another profile image, so that the corresponding points are found accurately. Since the profile can be extracted from an image, the profile pixel points in another profile image can be used as the centers to set up regions one by one to match the template, which ensures that the matching points are all on the grinding wheel profile and the matching accuracy is improved. Meanwhile, the operation efficiency is greatly improved because the number of points to be matched is less than that of whole image search. According to the principle mentioned above, a profile template matching based on the profile search algorithm is proposed to adapt to the mosaicing of grinding wheel profile images.

To construct a template based on the shape of the grinding wheel profile and search the profile pixels for the matching point, the profile needs to be extracted beforehand. The original grinding wheel images obtained by the CCD camera are binarized based on the Otsu algorithm, and profile extraction is based on the Canny operator, so that the pixel coordinates $I(x, y)$ of the profile images are obtained. On this basis, according to equations (1)–(3), a profile segment is extracted from the overlapping area in one of the mosaic images and the profile template is established. The process can be described as follows:

$$T_x(i, j) = M_x * I_{temp}(i, j) \quad (1)$$

$$T_y(i, j) = M_y * I_{temp}(i, j) \quad (2)$$

$$T(i, j) = T_x^2(i, j) + T_y^2(i, j) \quad (3)$$

where $I_{temp}(i, j) \in \Omega(p, q)$, $\Omega(p, q)$ is an $M \times N$ profile template whose center is $I(p, q)$, $*$ represents the convolution operation, and $T(i, j)$ represents the descriptor of pixel $I_{temp}(i, j)$. M_x and M_y , respectively, represent the horizontal mask and vertical mask of the Sobel operator:

$$M_x = \begin{bmatrix} 1 & 0 & -1 \\ 2 & 0 & -2 \\ 1 & 0 & -1 \end{bmatrix}, \quad M_y = \begin{bmatrix} 1 & 2 & 1 \\ 0 & 0 & 0 \\ -1 & -2 & -1 \end{bmatrix}. \quad (4)$$

The horizontal and vertical convolution of the profile can extract the profile variety characteristics in both the horizontal and vertical directions and highlight the profile features. Because the descriptor containing profile variety information can enhance the matching degree of target points in the process of image matching, the square sum of the horizontal and vertical convolution results is taken as the descriptor of the profile pixel.

Similarly, in the other mosaic image, the pixel coordinate of the profile is extracted and the profile descriptor is constructed by the Sobel operator convolution. According to the extracted profile information, the matched profile regions of the same size as the profile template are established by taking each profile pixel as the center. This is shown in equations (5)–(7):

$$R_x(i, j) = M_x * I_{obj}(i, j) \quad (5)$$

$$R_y(i, j) = M_y * I_{obj}(i, j) \quad (6)$$

$$R(i, j) = R_x^2(i, j) + R_y^2(i, j) \quad (7)$$

where $I_{obj}(i, j) \in \Omega(s, t)$ and $\Omega(s, t)$ is the $M \times N$ profile region to be matched whose center is $I(s, t)$. $R(i, j)$ represents the descriptor of the pixel $I_{obj}(i, j)$. $I(s, t)$ are the pixel coordinates of the profile.

Then, the matching similarity between the template and the target regions which center on the profile pixels is calculated. The similarity is calculated by spatial correlation in which the dot product of the profile template and target region is summed and normalized. As shown in equation (8):

$$S = \frac{\sum_{\Omega(p,q)} \sum_{\Omega(s,t)} T(i,j) \cdot R(i,j)}{\|T(i,j)\|_2 \cdot \|R(i,j)\|_2} \quad (8)$$

$$= \frac{\sum_{x=M/2}^{x+M/2} \sum_{y=N/2}^{y+N/2} T(i,j) \cdot R(i,j)}{\left[\sum_{x=M/2}^{x+M/2} \sum_{y=N/2}^{y+N/2} T^2(i,j) \cdot \sum_{x=M/2}^{x+M/2} \sum_{y=N/2}^{y+N/2} R^2(i,j) \right]^{1/2}}$$

The larger the correlation S , the higher the profile similarity. The point $I(s, t)$ corresponding to the maximum correlation of all profile points is the point which matches the template center $I(p, q)$. As described in section 2.1, the profile images of the grinding wheel are captured by moving the CCD camera along the X and Z axes. There is only a translation relationship between the profile images of the same cross-section, and the translation parameters can be determined based on the profile matching points between the images. The profile image mosaicing can therefore be realized.

According to equations (1)–(8), the profile template matching based on the profile search algorithm and the results of the grinding wheel profile image mosaicing are shown in

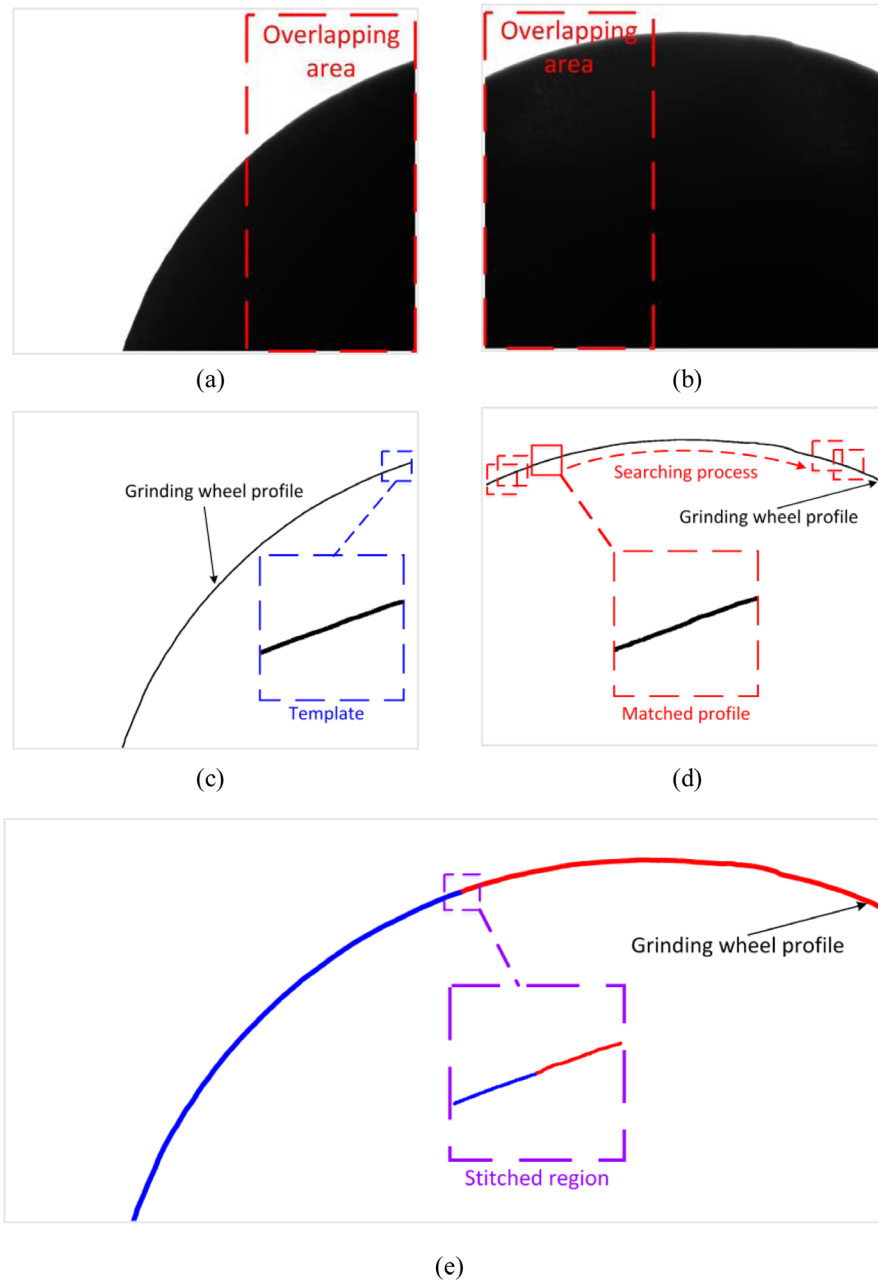


Figure 3. Profile template matching based on profile search algorithm: (a) image 1 to be mosaiced, (b) image 2 to be mosaiced, (c) establishing profile template, (d) searching for matching point, and (e) profile image mosaic result.

figure 3. The parameters of the grinding wheel profile image are shown in table 2. Figure 3(a) and (b) are two original images to be mosaiced and their overlapping area is 30% of the image area. The grinding wheel profile is extracted from the original images by image binarization and the Canny edge extraction method. Figure 3(c) shows the process of establishing the profile template in the overlapping area using equations (1)–(4). The template region is 200×200 pixels (about 1% of the image size) whose center is one of the profile points. Figure 3(d) is the searching process of template matching along the profile in the other image. Using equations (4)–(7), the same size regions to be matched are established by taking

Table 1. Image mosaic accuracy and efficiency experimental parameters.

Parameters	Value
Size of CCD sensor (inch)	2/3
Lens magnification	4 ×
Image pixel size (pixel)	2056 × 2452
Moving interval in X-direction	0.5 mm
Total number of images	7
Total number of image groups	5
The number of images in each group	3
Overlapping area of left and right images	45.5%

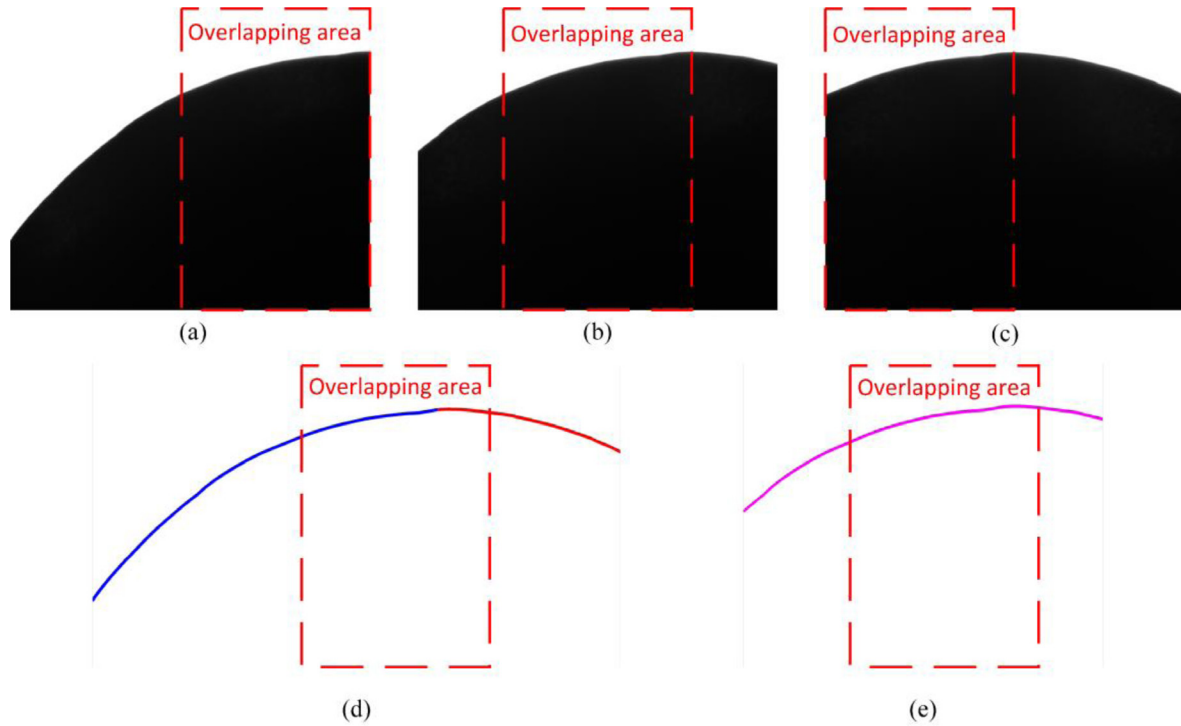


Figure 4. Example of accuracy and efficiency experiment image group: (a) left mosaic image, (b) intermediate actual profile image, (c) right mosaic image, (d) stitched profile, and (e) actual profile.

the profile pixels as centers. The correlations between each searching regions and the template are calculated by equation (8). After finding the maximum correlation of the points, the matching process is finished and the matching points of the two images are found. Thus, the translation parameters can be obtained and the two profile images are mosaiced by translation. Figure 3(e) is the final result of the grinding wheel image mosaicing. The template center and the matching region center coincide and the remaining parts of the two images are mosaiced into a more complete profile image.

The image mosaic algorithm obtains the complete information to be measured based on the image coordinate system, which means that the accuracy of the image mosaic directly affects the final measurement accuracy. To achieve the complete acquisition and accurate measurement of the grinding wheel profile, the accuracy of the image mosaic algorithm must be guaranteed. In addition, in the measurement process, there is more than one image to be mosaiced, and the mosaicing efficiency is also an issue to be considered.

To confirm the validity of the profile template matching based on the profile search algorithm, it was compared with common image mosaicing algorithms, such as image mosaic based on grayscale matching [21, 22] (pixel-based mosaicing), image mosaic based on shape template matching [23] (contour-based mosaicing) and the scale-invariant feature transform (SIFT) [24] (low-level feature-based mosaicing) image mosaic algorithm, which are image mosaicing algorithms based on different image matching principles for different image registration occasions.

Above all, an available image mosaic algorithm should satisfy high accuracy. In order to compare the image mosaic

accuracy of different algorithms, the following experiment was designed: a 5 mm diameter hemispherical grinding wheel was measured and the spherical crown images were captured. The experimental parameters are shown in table 1. The actual size of the FOV for each image is about 2.2 mm × 1.76 mm, and every image was captured by moving the X-direction translation stage 0.5 mm at a time. Seven images were captured to cover a cross-sectional profile, and every three images composed an image group, so five image groups were obtained. In each group of images, the left and right images are two mosaicing images with about 45.5% overlapping area, and the intermediate image contains the true profile of the overlapping area. Figure 4 shows one image group as example. Figures 4(a) and (c) are two mosaicing images and figure 4(b) is the intermediate image. Figure 4(d) shows the stitching result of figures 4(a) and (c). Figure 4(e) is the true profile extracted directly from figure 4(b). Five image groups, mentioned above, were processed by this method. The similarities between the stitching profiles and the true profiles in the overlapping area were calculated by equation (9).

$$R = \frac{\sum_{m=1}^M \sum_{n=1}^N S(m, n) \times T(m, n)}{\sqrt{\sum_{m=1}^M \sum_{n=1}^N S^2(m, n)} \sqrt{\sum_{m=1}^M \sum_{n=1}^N T^2(m, n)}} \quad (9)$$

where $S(m, n)$ is the pixel gray value of the stitching profile in the overlapping area and $T(m, n)$ is the pixel gray value of the true profile in the overlapping area. M and N represent the length and width of the overlapping area, respectively.

Apparently, the higher the similarity is, the more consistent the stitching profile is with the true profile, which means the algorithm has higher accuracy. The normalized similarities between the profiles stitched by different algorithms and the

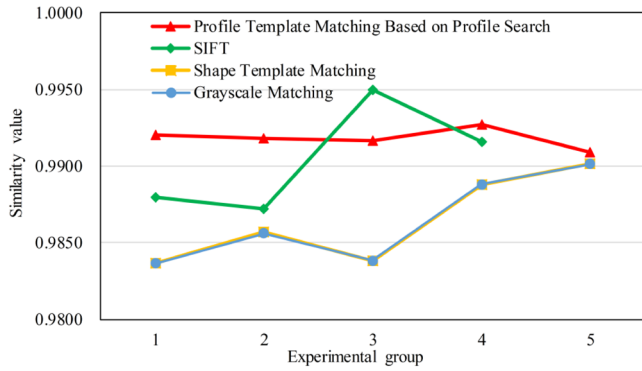


Figure 5. Similarity of different image mosaic algorithms.

true profile of overlapping area are calculated by equation (9), and the results of the five image groups are shown in figure 5. As shown in this figure, it is obvious that the similarities of the image mosaic based on grayscale matching and shape template matching are very close, and they are all lower than those of the other two algorithms. The principle of grayscale matching is to calculate the gray value similarity between the ‘windows’ in the two mosaicing images for each shift. The gray value is easily affected by the environment, such as illumination changes in matching images, reducing the accuracy of matching point search, and thus affecting the image mosaic accuracy. The image mosaic based on shape template matching lacks recognition of the grinding wheel profile position. The matching points may not be points on the profile, therefore the accuracy is limited. The profile similarities of the SIFT operator are slightly higher, but except for the third experiment, its similarities are lower than those of the proposed algorithm. In addition, the SIFT algorithm fails in the fifth experiment because there are not enough key points detected in the grinding wheel profile images which results in the failure of the image mosaic. In this study, the images mainly contain white background and grinding wheel profile shadow; the proposed algorithm can extract enough profile information for template construction and the searching process guarantees that the matching points are all on the profile. Thus, the profile template matching based on the profile search algorithm can find the matching points between images more accurately, and make the subsequent image mosaic more accurate. As can be seen from figure 5, the image mosaic using profile template matching based on the profile search algorithm has the highest similarities in the five groups of experiments, which means it has the highest image mosaic accuracy among the four algorithms.

The robustness can also be shown from the above experimental results. Under the same experimental conditions, the similarity value of the proposed algorithm is more stable than those of other algorithms and there is no failure or obvious fluctuation. The characteristic of gray matching that is easily affected by external conditions is also reflected in terms of robustness. The similarity changes obviously and has fluctuations. Shape template matching also has problems that mainly result from the image noises. Uncertain image noises in the edge area could seriously affect the shape extraction and

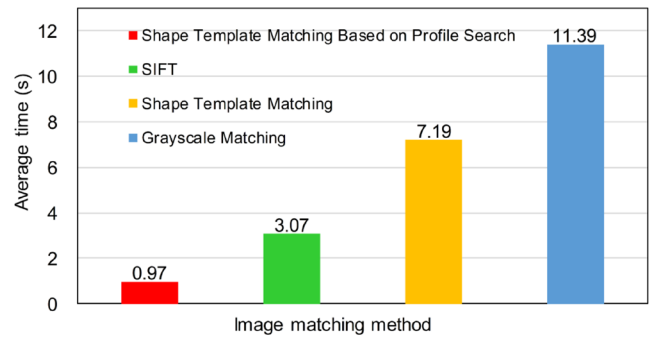


Figure 6. Average operation time of different image mosaic algorithms.

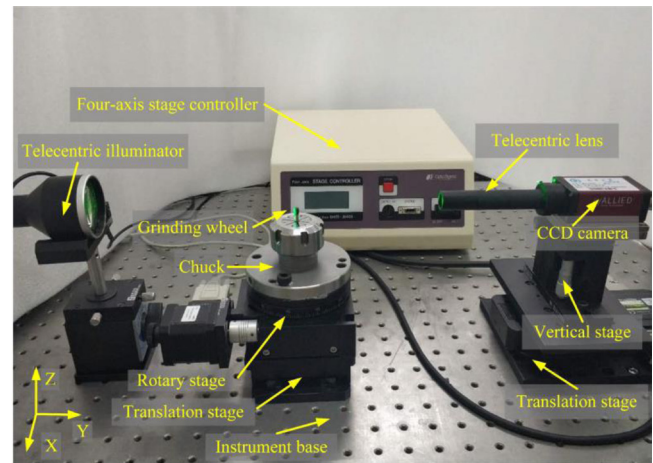


Figure 7. The grinding wheel profile measurement system.

template establishment. Therefore, it is difficult to guarantee the stability of these two algorithms. In this study, the stability of the SIFT operator depends on the number of key points constructed in the profile images. When enough key points can be extracted, the mosaic accuracy will be relatively high, such as in experimental group 3. In contrast, when the number of key points is insufficient, the mosaic accuracy can be low, and the image mosaic can even fail, such as experimental group 5. Thus, the SIFT algorithm cannot guarantee robustness for the grinding wheel profile image mosaic. The profile template matching based on the profile search algorithm enhances the characterization of profiles and uses profile characteristics to establish a template, which can effectively overcome image noises and accurately find the profile similar to the template. According to the experimental results, the proposed algorithm has stable similarity results above 0.99 and no failure. Therefore, the profile template matching based on the profile search algorithm also has an advantage over other algorithms in the robustness of grinding wheel profile image mosaic.

Figure 6 shows the average operation time of different image mosaic algorithms for five image groups. As shown in figure 6, the profile matching based on the profile search algorithm has the shortest operation time for each image group, which means that it has better computational efficiency compared with other image mosaic algorithms. This is because searching profile pixels for the matching point greatly reduces the number of

Table 2. Image acquisition conditions and parameters of the measured grinding wheels.

Parameters	Value	
Image pixel size (pixel)	2056 × 2452	
Size of CCD sensor (inch)	2/3	
Lens magnification	4 ×	
Scale of pixel size and actual size in vertical direction	1 : 0.8604	
Scale of pixel size and actual size in horizontal direction	1 : 0.8626	
Template size (pixel)	200 × 200	
The distance of every movement in X direction (mm)	0.6 mm	
The distance of every movement in Z direction (mm)	0.35 mm	
Ratio of overlapping area to image area	20% – 30%	
Accuracy of X-direction translation table (μm)	10	
Accuracy of Z-direction translation table (μm)	10	
Accuracy of Y-direction translation table (μm)	5	
Cylindrical grinding wheel	Grit size	W40
	Size of abrasive grain (μm)	28–40
	Diameter (mm)	10
	Grinding length (mm)	12
Hemispherical grinding wheel	Grit size	W5
	Size of abrasive grain (μm)	3.5–5
	Radius (mm)	2.5

target points to be processed. By contrast, grayscale matching and shape template matching respectively use pixel gray level values and shape information in a small ‘window’ to search a large area in a target image to be matched, for the maximum similarity. A large number of the non-profile points search processes are time-consuming. Thus, the efficiency of these two methods is lower. SIFT operators need to construct scale-space and their method to define key point descriptors is more complex than the profile template matching based on the profile search algorithm; the processing efficiency is affected and slightly lower than the proposed algorithm.

Therefore, according to the characteristics of grinding wheel profile images, the profile template matching based on the profile search algorithm can ensure higher image mosaicing accuracy and realize quicker profile image mosaicing. Compared with the other image mosaic algorithms, it is more suitable for the grinding wheel profile image mosaic.

3. Experiments and discussion

In order to validate the proposed grinding wheel profile measurement method based on image mosaic, as shown in figure 7, a measurement system for a grinding wheel profile was established and employed to autofocus a grinding wheel profile and acquire profile images. The axis of the grinding wheel is perpendicular to the base plane, and the optical axis of the imaging system is parallel to the base plane, so their axes are perpendicular to each other. The grinding wheel was fixed by an ER chuck and centered using an inductance displacement sensor. The imaging system axis was also aligned. When moving along the Y direction, the displacements of the lens in the X and Z direction were measured by an inductive displacement sensor, and corresponding position adjustment

was carried out to eliminate the X and Z direction displacement of the imaging system in the movement along the Y axis. In this way, the alignment between the optic axis and the grinding wheel axis was handled. Through the movement of the X-direction translation stage and Z-direction vertical stage, the grinding wheel profile was moved into the FOV. Autofocus [13] of the grinding wheel profile was realized by moving the CCD camera along the optical axis (Y axis) and searching for the maximally sharp position in the image sequence. Then, through X direction and Z direction translation, different section images of the grinding wheel profile could be obtained. By rotating the grinding wheel and repeating the above steps, profiles at different angles can be measured.

The profile images with overlapping areas are matched and stitched into a complete profile using profile template matching based on the profile search algorithm. According to the calibration results between the pixel size and actual size, actual coordinates and dimensions of the grinding wheel profile could be obtained.

In this study, two different grinding wheels were measured using the proposed method: a cylindrical grinding wheel and hemispherical grinding wheel. The parameters of the grinding wheels and measurement conditions are given in table 2. The parameters of the image mosaic were selected according to the size of the FOV and the number of mosaic images depended on the size of the grinding wheels. The theoretical size of the 2/3-inch CCD sensor is about 8.8 mm × 6.6 mm. Considering that the magnification of the lens is 4×, the actual imaging area is about 2.2 mm × 1.65 mm. To obtain profile images whose overlapping areas are about 20%–30% of the whole image size, the distances of every movement in the X direction and Z direction are 1.6 mm and 1.3 mm respectively. The grinding length of the cylindrical grinding wheel is 12 mm

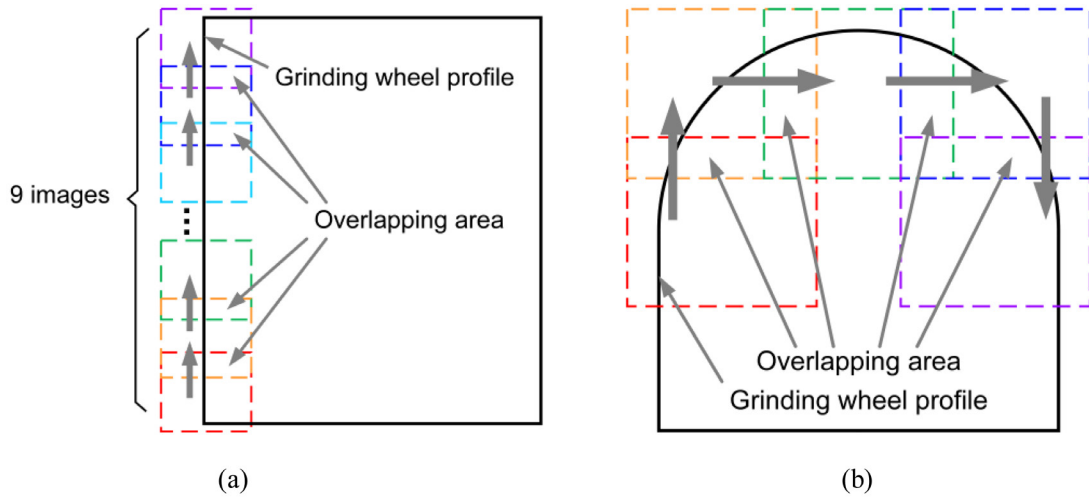


Figure 8. Schematic diagram of mosaic images acquisition: (a) mosaic images of cylindrical grinding wheel, and (b) mosaic images of hemispherical grinding wheel.

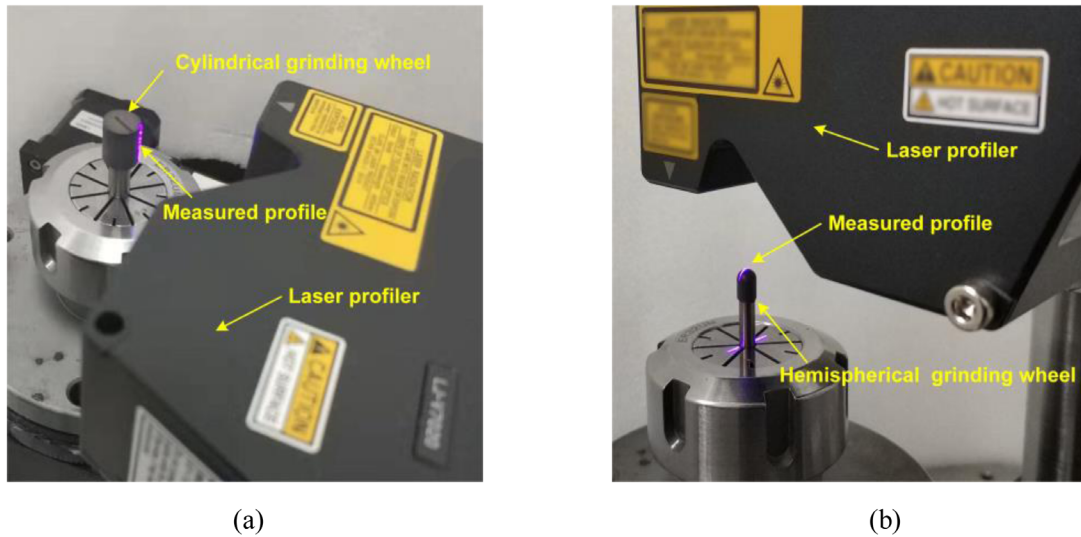


Figure 9. Laser profiler measuring grinding wheel profile: (a) profiler measuring cylindrical grinding wheel, and (b) profiler measuring hemispherical grinding wheel.

Table 3. Main measuring characteristics of the laser profiler.

Feature	Value
Measurement range (height)	± 2.3 mm
Measurement range (width)	7 mm
Profile data interval (width)	10 μ m
Measurement accuracy	± 3 μ m
Maximum measured inclination	65°

nominally, therefore, nine images are needed to cover its profile, as shown in figure 8(a). Likewise, the nominal radius of the hemispherical grinding wheel is 2.5mm, and five images are needed to cover its profile, as shown in figure 8(b).

The profiles at different angles of the two grinding wheels could be measured by rotating the grinding wheel. In the experiment, profiles of five positions were selected at equal angle interval and measured for the cylindrical grinding wheel and hemispherical grinding wheel respectively. The sampling positions are shown in figure 10(f) for the cylindrical grinding

wheel and figure 11(f) for the hemispherical grinding wheel. The measurement results of the proposed algorithm are shown as blue lines in figures 10(a)–(e) and 11(a)–(e).

A commercial 2D laser profiler (Keyence LJ-V7020) was employed to measure the grinding wheel profiles in the same positions to validate the feasibility of the method and the accuracy of the measurement results. The comparative experimental device and measurement process are shown in figure 9. The main working features of this profiler are shown in table 3.

Since the measurement range in width and the maximum measured inclination of the profiler are limited, this device cannot measure the complete profile. In order to compare the profile results measured by the proposed method and laser profiler, the profiles in the profiler measurement range were compared.

The profiler measurement results of the cylindrical grinding wheel and the hemispherical grinding wheel are shown as red lines in figures 10(a)–(e) and 11(a)–(e), respectively. The two sets of data have been unified in the same coordinate system. For the cylindrical grinding wheel, the root mean

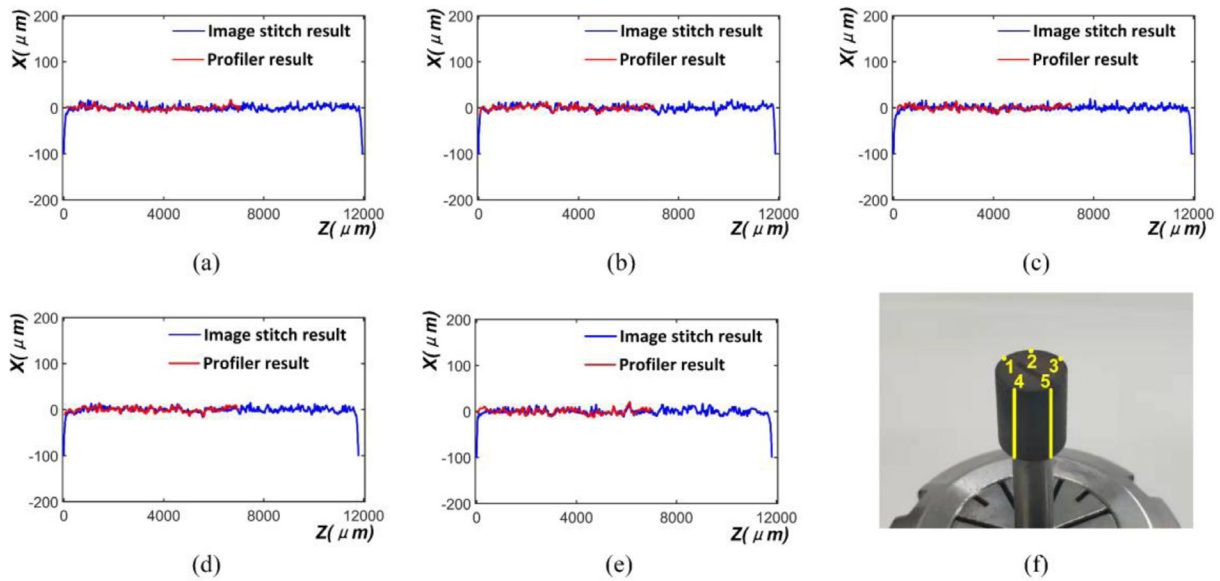


Figure 10. Measuring positions and corresponding results of the cylindrical grinding wheel: (a) position 1 results, (b) position 2 results, (c) position 3 results, (d) position 4 results, (e) position 5 results, and (f) five measuring positions.

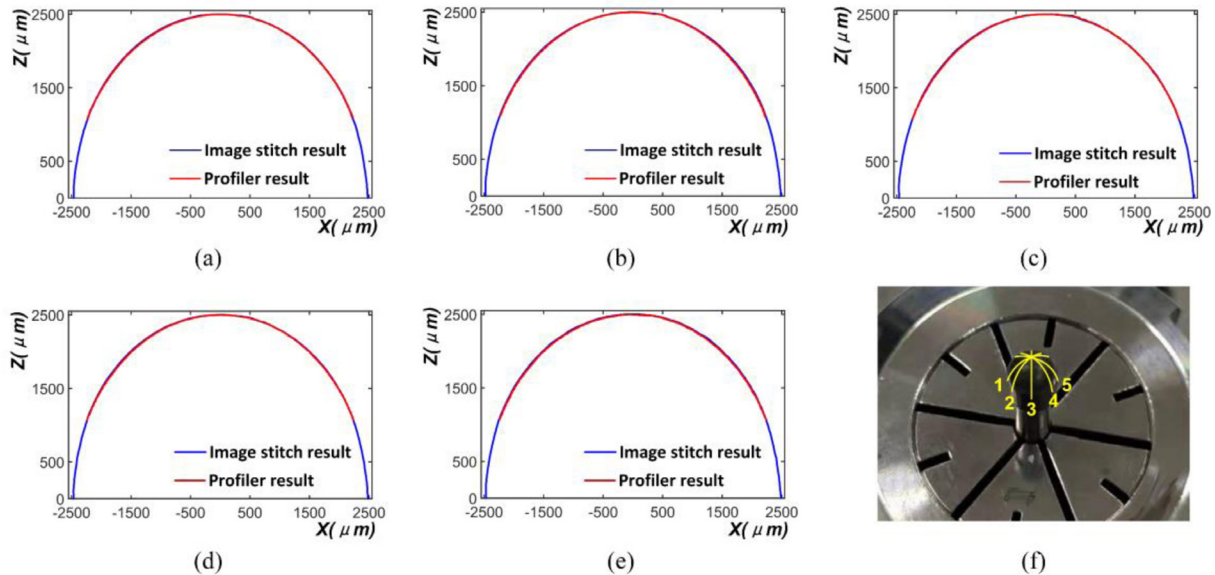


Figure 11. Measuring positions and corresponding results of hemispherical grinding wheel: (a) position 1 results, (b) position 2 results, (c) position 3 results, (d) position 4 results, (e) position 5 results, and (f) five measuring positions.

Table 4. Cylindrical grinding wheel RMSE between two profiles.

Measuring positions	RMSE (μm)
1	4.6159
2	5.0105
3	4.3579
4	4.7050
5	5.0972

squared error (RMSE) between the two profiles was calculated. The results are shown in table 4. Compared with the nominal radius of the cylindrical grinding wheel, the profile measurement deviation ranges from 0.08% to 0.1%. For the hemispherical grinding wheel, the coordinate deviation of the

circle center in the direction of the X-axis and Z-axis were calculated, as well as the radius measurement deviation. The results are shown in table 5, the deviation of the center position is between $\pm 3 \mu\text{m}$, and the radius deviation is below $3 \mu\text{m}$, which is about 0.1% of the nominal radius.

The results indicate that the measurement results of the grinding wheel profile based on the image mosaic have good consistency with the profiler results. However the profiler measurement range is limited in width and inclination, and it is difficult to obtain the complete measured profile, while the proposed method in this study can be adapted to grinding wheels with different shapes and obtain the complete target profile. Further analyzing the measurement deviation, the diamond grains distributed on the surface of the grinding wheel

Table 5. Hemispherical grinding wheel center position and radius deviation.

Measuring positions	Center deviation (X) (μm)	Center deviation (Z) (μm)	Radius deviation (μm)
1	-2.1080	1.3407	2.2054
2	0.2970	1.2566	2.5858
3	1.9807	-2.0109	2.3952
4	1.2340	-0.6252	2.3040
5	-1.0722	0.0264	2.8617

could cause a strong reflection inducing measurement error for the laser profiler and these positions would cause relatively high deviation between the two profiles. In addition, the sampling points interval of the laser profiler is 10 μm , while the interval of profile points acquired from the images in this study is below 1 μm . This means that the profile acquired by the image mosaic contains more profile information, such as some peaks and grooves. However, the 2D laser profiler would probably miss these positions due to its sampling interval, which could also be the source of deviation.

The measurement results are consistent with the results of the 2D laser profiler. Therefore, the grinding wheel profile measuring method based on image mosaic is feasible and suitable. The profile template matching based on the profile search algorithm achieves an accurate image mosaic of the grinding wheel profile, and solves the limitation of wheel profile measurement based on machine vision caused by the size of field of view and the range of the instrument, so that it can obtain a complete grinding wheel profile while retaining high resolution. The proposed method realizes non-contact measurement of the grinding wheel profile and efficient acquisition of grinding wheel profile information compared with contact measurement, as well as avoiding wear to the grinding wheel surface. In addition, direct measurement of the grinding wheel profile can more truly reflect the grinding wheel profile at different sections, and the actual grinding process in indirect measurement can be avoided. Based on the profile recognition and matching of the proposed method, the measurement of grinding wheel profile is not limited to the shape and size of grinding wheel. For the measurement of different grinding wheels and their different sections, this method has better adaptability. Moreover, compared with a contact measuring instrument and non-contact optical profiler, the system based on the proposed method has a simpler structure and lower cost.

4. Conclusion

In the grinding process, the profile of the grinding wheel directly affects the shape accuracy of the workpiece. Therefore, accurate measurement of the grinding wheel profile is helpful in evaluating the grinding wheel processing accuracy, detecting wear and compensating for machining errors. In this paper, a novel grinding wheel profile measurement method is investigated.

1. A profile template matching based on the profile search algorithm is proposed in order to realize a quick and accurate image mosaic of an overlapping small field of view profile images. The method establishes a shape template of the overlapping profile according to the characteristics of the grinding wheel profile images and only searches the recognized profile for matching points. This method effectively avoids the searching process of non-profile points and improves the accuracy of profile matching.
2. A grinding wheel profile measurement method based on machine vision and image mosaicing is developed, and a measurement system is established to realize the profile measurement of grinding wheels with different shapes. Compared with the commercial laser profiler, for a cylindrical grinding wheel, the RMSE between the profile results is 0.08%–0.1% of the nominal radius, and for the hemispherical grinding wheel, the center position deviation is $\pm 3 \mu\text{m}$, and the radius deviation is below 0.1% of the nominal radius.

The method and the system in this paper is not limited to measuring cylindrical grinding wheels and hemispherical grinding wheels. Saucer grinding wheels and grinding wheels of other shapes can also be measured. Because working parts of some types of grinding wheels, such as the arc edge of saucer grinding wheel, are small enough in size that they can be captured completely in the field of view, they may not need image mosaic algorithms. On the basis of the method in this paper, future research could combine grinding wheel rotational sampling and 2D to 3D coordinate transformation, and 3D profile measurement of a grinding wheel could be realized. Combined with grinding wheel surface topography measurement [7–10, 14], more complete evaluation of processing accuracy and grinding performance can be achieved.

Acknowledgment

This work was supported by The National Key Research and Development Program of China (No. 2018YFB1107605) and The Natural Science Foundation of China (Nos. 51875405 and 51375336).

ORCID iDs

Tianyi Li  <https://orcid.org/0000-0001-8991-835X>

References

- [1] Qiu Z J, Liu C C, Wang H R, Yang X, Fang F Z and Tang J J 2016 Crack propagation and the material removal mechanism of glass–ceramics by the scratch test *J. Mech. Behav. Biomed. Mater.* **64** 75–85
- [2] Huang H, Chen W K and Kuriyagawa T 2007 Profile error compensation approaches for parallel nanogrinding of aspherical mould inserts *Int. J. Mach. Tools Manuf.* **47** 2237–45

- [3] Xu L M, Fan F, Zhang Z, Chao X J and Niu M 2019 Fast on-machine profile characterization for grinding wheels and error compensation of wheel dressing *Precis. Eng.* **55** 417–25
- [4] Zhang Z *et al* 2017 High-performance grinding of a 2-m scale silicon carbide mirror blank for the space-based telescope *Int. J. Adv. Manuf. Technol.* **89** 463–73
- [5] Chen W K, Kuriyagawa T, Huang H and Yosihara N 2005 Machining of micro aspherical mould inserts *Precis. Eng.* **29** 315–23
- [6] Loizou J *et al* 2015 Automated wear characterization for broaching tools based on machine vision systems *J. Manuf. Syst.* **37** 558–63
- [7] Kaplonek W, Lukianowicz C and Nadolny K 2012 Methodology of the assessment of the abrasive tool's active surface using laser scatterometry *Trans. Can. Soc. Mech. Eng.* **36** 49–66
- [8] Darafon A, Warkentin A and Bauer R 2013 Characterization of grinding wheel topography using a white chromatic sensor *Int. J. Mach. Tools Manuf.* **70** 22–31
- [9] Boaron A and Weingaertner W L 2018 Dynamic in-process characterization method based on acoustic emission for topographic assessment of conventional grinding wheels *Wear* **406–7** 218–29
- [10] Brown C A *et al* 2018 Multiscale analyses and characterizations of surface topographies *CIRP Ann.* **67** 839–62
- [11] Su J C and Tarng Y S 2006 Measuring wear of the grinding wheel using machine vision *Int. J. Adv. Manuf. Technol.* **31** 50–60
- [12] Chen T H, Chang W T, Shen P H and Tarng Y S 2010 Examining the profile accuracy of grinding wheels used for microdrill fluting by an image-based contour matching method *Proc. Inst. Mech. Eng. B* **224** 899–911
- [13] Magdziak M and Wdowik R 2015 Contact and non-contact measurements of grinding pins *MATEC Web of Conf.* p 35 (<https://doi.org/10.1051/mateconf/20153502004>)
- [14] Tang J J, Qiu Z J and Li T Y 2019 A novel measurement method and application for grinding wheel surface topography based on shape from focus *Measurement* **133** 495–507
- [15] Valiño G, Wdowik R, Misiura J and Zapico P 2017 Non-contact measurement of grinding pins by means of a 2D laser micrometer *Proc. Manuf.* **13** 534–41
- [16] Young H T and Chen D J 2006 Online dressing of profile grinding wheel *Int. J. Adv. Manuf. Technol.* **27** 883–8
- [17] Xu L M, Niu M, Zhao D, Xing N B and Fan F 2019 Methodology for the immediate detection and treatment of wheel wear in contour grinding *Precis. Eng.* **60** 405–12
- [18] He J, Zhou R Z and Hong Z L 2003 Modified fast climbing search auto-focus algorithm with adaptive step size searching technique for digital camera *IEEE Trans. Consum. Electron.* **49** 257–62
- [19] Ghosh D and Kaabouch N 2016 A survey on image mosaicing techniques *J. Vis. Commun. Image Represent.* **34** 1–11
- [20] Pandey A and Pati U C 2019 Image mosaicing: a deeper insight *Image and Vision Computing* **89** 236–57
- [21] Barnea D I and Silverman H F 1972 A class of algorithms for fast digital image registration *IEEE Trans. Comput.* **C-21** 179–86
- [22] Ghannam S and Abbott A 2013 Cross correlation versus mutual information for image mosaicing *Int. J. Adv. Comput. Sci. Appl.* **4** 94–102
- [23] Islam B and Kabir J 2013 A new feature-based image registration algorithm *Comput. Technol. Appl.* **4** 79–84
- [24] Lowe D 2004 Distinctive image features from scale-invariant keypoints *Int. J. Comput. Vis.* **60** 91–110